^{99}Tc and Re Incorporated into Metal Oxide Polyoxometalates: Oxidation State Stability Elucidated by Electrochemistry and Theory

Donna McGregor,[#,†,‡] Benjamin P. Burton-Pye,[#,†] Israel M. Mbomekalle,[†,∥] Pablo A. Aparicio,[§] Susanna Romo,[§] Xavier López,[§] Josep M. Poblet,[§] and Lynn C. Francesconi*[†,‡]

[†]Hunter College, City University of New York, 695 Park Avenue, New York, New York 10065, United States
[‡]Graduate Center, City University of New York, New York 10016, United States
[§]Departament de Química Física i Inorgànica, Universitat Rovira i Virgili, Marcel·li Domingo s/n, 43007 Tarragona, Spain

S *Supporting Information*

ABSTRACT: The radioactive element technetium-99 (^{99}Tc, half-life = 2.1×10^5 years, β^- of 253 keV), is a major byproduct of ^{235}U fission in the nuclear fuel cycle. ^{99}Tc is also found in radioactive waste tanks and in the environment at National Lab sites and fuel reprocessing centers. Separation and storage of the long-lived ^{99}Tc in an appropriate and stable waste-form is an important issue that needs to be addressed. Considering metal oxide solid-state materials as potential storage matrixes for Tc, we are examining the redox speciation of Tc on the molecular level using polyoxometalates (POMs) as models. In this study we investigate the electrochemistry of Tc complexes of the monovacant Wells−Dawson isomers, α_1-$P_2W_{17}O_{61}{}^{10-}$ ($\alpha1$) and α_2-$P_2W_{17}O_{61}{}^{10-}$ ($\alpha2$) to identify features of metal oxide materials that can stabilize the immobile Tc(IV) oxidation state accessed from the synthesized Tc(V)O species and to interrogate other possible oxidation states available to Tc within these materials. The experimental results are consistent with density functional theory (DFT) calculations. Electrochemistry of $K_{7-n}H_n[Tc^VO(\alpha_1\text{-}P_2W_{17}O_{61})]$ (**Tc^{V}O-$\alpha1$**), $K_{7-n}H_n[Tc^VO(\alpha_2\text{-}P_2W_{17}O_{61})]$ (**Tc^{V}O-$\alpha2$**) and their rhenium analogues as a function of pH show that the Tc-containing derivatives are always more readily reduced than their Re analogues. Both Tc and Re are reduced more readily in the lacunary $\alpha1$ site as compared to the $\alpha2$ site. The DFT calculations elucidate that the highest oxidation state attainable for Re is VII while, under the same electrochemistry conditions, the highest oxidation state for Tc is VI. The $M^V \rightarrow M^{IV}$ reduction processes for **Tc^{V}O-$\alpha1$** are not pH dependent or only slightly pH dependent suggesting that protonation does not accompany reduction of this species unlike the **M^{V}O-$\alpha2$** (M = ^{99}Tc, Re) and **Re^{V}O-$\alpha1$** where $M^{V/IV}$ reduction process must occur hand in hand with protonation of the terminal M=O to make the π^*(M=O) orbitals accessible to the addition of electrons. This result is consistent with previous extended X-ray absorption fine structure (EXAFS) and X-ray absorption near edge structure (XANES) data that reveal that the Tc^V is "pulled" into the -$\alpha1$ framework and that may facilitate the reduction of **Tc^{V}O-$\alpha1$** and stabilize lower Tc oxidation states. This study highlights the inequivalency of the two sites, and their impact on the chemical properties of the Tc substituted in these positions.
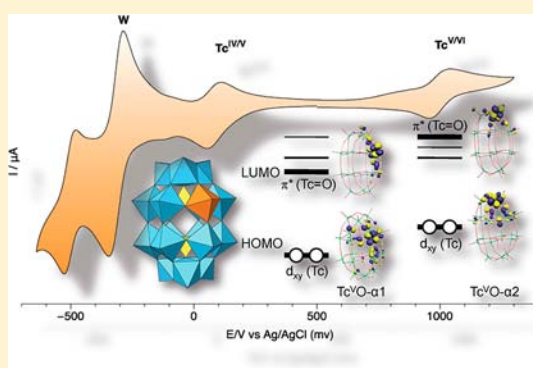
■ INTRODUCTION

The isotope ^{99}Tc (half-life = 2.1×10^5 years, β^- of 253 keV) is a major byproduct in the nuclear fuel cycle and constitutes ~6% of the fission yield. ^{99}Tc is also found in radioactive waste tanks from defense activities of the 1940s and 1950s. In some cases, because of tank leakage, ^{99}Tc is found in the environment—in water and soils at National Lab sites and fuel reprocessing centers.[1−11] Regardless of the source, separation and storage of the long-lived ^{99}Tc in an appropriate and stable waste-form is an important issue that needs to be addressed.[12]

^{99}Tc possesses extensive redox chemistry with compounds found in oxidation states of −1 to +7. ^{99}Tc is often found in its highest oxidation state Tc(VII), where it exists primarily as the pertechnetate anion (TcO_4^-). This anion is the most stable

form of Tc under basic conditions and is extremely mobile within the environment.[5,6] Most waste sequestration and immobilization strategies involve reduction of TcO_4^- to Tc(IV) in the form of $TcO_2 \cdot nH_2O$ that is relatively immobile.[13−16] To formulate robust, manageable waste remediation strategies it is important to understand the fundamental factors that influence the redox characteristics and stability of technetium within potential storage materials. Considering metal oxide solid-state materials as potential storage matrixes for Tc, we are examining the speciation of Tc within metal oxide matrixes on the molecular level using polyoxometalates (POMs) as models. POMs[17−20] possess surface binding sites as well as "defect" sites

with varying electronic and steric properties and "loading capacities". The coordination chemistry and redox speciation can be probed by a number of species-specific techniques to obtain a molecular level understanding that can be related to solid-state materials. We have found also that POMs can serve to transfer electrons to TcO_4^- to reduce $Tc(VII)$ to lower valent Tc that can be sequestered by the POM.[21]

In this study we employ the well-known phosphorus–tungsten derivatives of the polyanion α-$P_2W_{18}O_{62}^{6-}$, specifically the lacunary derivatives α_1-$P_2W_{17}O_{61}^{10-}$ and α_2-$P_2W_{17}O_{61}^{10-}$. These lacunary ions are achieved through removal of one "belt" tungsten (a tungsten from one of the two equatorial W_6 rings) or one "cap" tungsten (a tungsten from one of the two polar W_3 regions) respectively (Figure 1). The resulting vacancies
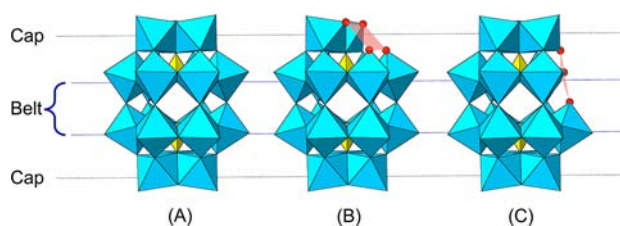

Figure 1. Plenary Wells−Dawson ion and lacunary Wells−Dawson isomers shown in polyhedral representation. (A) $(\alpha$-$P_2W_{18}O_{62})^{6-}$ is the "plenary" or parent Wells−Dawson ion, about 1.2 nm in length and 0.6 nm width; (B) removal of a "cap" W from the plenary Wells−Dawson structure gives the "lacunary" $(\alpha_2$-$P_2W_{17}O_{61})^{10-}$ isomer; (C) removal of a "belt" W from the plenary Wells−Dawson gives the $(\alpha_1$-$P_2W_{17}O_{61})^{10-}$ isomer. The terminal oxygen atoms in the defects are shown in red. The light red shading outlines the defects and does not reflect coordination of metal ions into the defect. Tc^VO coordinates into the defect in a distorted octahedral fashion with a $Tc{=}O$ terminal bond. The defect structures possess distinct and different electronic and steric features that impact chemical and redox speciation of ^{99}Tc.

provide excellent binding sites for metal ions and have very distinct and different steric and electronic properties.[22−27] These properties can be exploited to probe both the coordination and the redox properties of metals incorporated into the binding sites. We have reported a full detailed synthesis and characterization of $K_{7-n}H_n[Tc^VO(\alpha_1$-$P_2W_{17}O_{61})]$ (**Tc^VO-$\alpha1$**), $K_{7-n}H_n[Tc^VO(\alpha_2$-$P_2W_{17}O_{61})]$ (**Tc^VO-$\alpha2$**), $K_{7-n}H_n[Re^VO$-$(\alpha_1$-$P_2W_{17}O_{61})]$ (**Re^VO-$\alpha1$**), and $K_{7-n}H_n[Re^VO(\alpha_2$-$P_2W_{17}O_{61})]$ (**Re^VO-$\alpha2$**) along with preliminary electrochemistry results at pH 5.[27]

The aim of this study is to understand the properties of metal oxide materials that can potentially stabilize Tc. In general, the low valent $Tc(IV)$ oxidation state is targeted as it is considered immobile especially as $Tc^{IV}O_2$ compared to the very mobile pertechnetate anion, TcO_4^-. To achieve this aim, we conducted a study of the conditions required to stabilize Tc as $Tc(IV)$ within the α_1-$P_2W_{17}O_{61}^{10-}$ (**$\alpha1$**) and α_2-$P_2W_{17}O_{61}^{10-}$ (**$\alpha2$**) POMs. The **Tc^VO-$\alpha1$** and **Tc^VO-$\alpha2$** are excellent starting points as the Tc^{IV} state can be accessed by electrochemistry. Comparison of the lowest unoccupied molecular orbitals (LUMOs) derived from electrochemistry can inform on the ease of the $Tc^{V/IV}$ reduction, evaluate the stability of the Tc^{IV} within the POMs and interrogate other possible oxidation states available to Tc within these POMs. Examination of redox potential as a function of pH allows us to investigate the impact of protonation on speciation of **M^VO-$\alpha1$** and **M^VO-$\alpha2$** (M = Tc, Re).

Theory is most important to understand the trends observed in the electrochemistry. For medium- to large-sized compounds, such as POMs, density functional theory (DFT) calculations are known to give an accurate quantum-based view of the molecular properties. They provide an understanding of the relative stability of compounds (including isomers), binding modes, oxidation states, protonation states, and so forth,[28,29] as well as the useful molecular orbital (MO) vision.

We include a detailed DFT study on different oxidation states of ^{99}Tc and Re within **$\alpha1$** and **$\alpha2$**. In each case the structural parameters, energies and electron densities were analyzed to determine the theoretical redox behavior. The theory and the experimental electrochemistry reported here and X-ray Absorption Spectroscopy (XAS) reported previously[27] provide insight into the relationship between the electronic and the steric environments of the two isomeric POMs and the redox behavior of Tc. The theory and experimental treatment should provide an understanding of the requirements of metal oxide defects for promoting stability of low valent technetium.

We also consider Re in this study. Re, the third row congener of Tc, is widely used as a nonradioactive surrogate for Tc because it possesses similar atomic radii, the same number of d electrons available for bonding, and a similarly wide range of oxidation states. However, there are subtle but distinct differences between the reactivity, stability, and redox behavior of Tc and Re complexes.[30−33] These differences can impact the efficacy of Re as a true chemical surrogate for Tc. Examining both Tc and Re concomitantly presents the opportunity to identify the similarities and differences between these elements.

■ EXPERIMENTAL SECTION

General Procedures. ^{99}Tc is a weak β- emitter with a half-life of 2.1×10^5 years. All reported Tc syntheses were performed in an appropriately equipped lab approved for the use of low-level radioactivity. Suitable radioactive material handling procedures were employed. All materials were purchased as reagent grade and used without further purification. Water was obtained using a Millipore Direct Q5 system (conductivity = 18 m Ω). The aqueous soluble α_1-$P_2W_{17}O_{61}^{10-}$ (**$\alpha1$**) and α_2-$P_2W_{17}O_{61}^{10-}$ (**$\alpha2$**) ligands were prepared as reported in the literature.[34,35] The $K_{7-n}H_n[Re^VO(\alpha_2$-$P_2W_{17}O_{61})]$ (**Re^VO-$\alpha2$**), $K_{7-n}H_n[Re^VO(\alpha_1$-$P_2W_{17}O_{61})]$ (**Re^VO-$\alpha1$**), $K_{7-n}H_n[Tc^VO(\alpha_2$-$P_2W_{17}O_{61})]$ (**Tc^VO-$\alpha2$**), and $K_{7-n}H_n[Tc^VO(\alpha_1$-$P_2W_{17}O_{61})]$ (**Tc^VO-$\alpha1$**) were prepared as previously described.[27,36]

Collection of Electrochemical Data. Electrochemical data were obtained using a BAS Voltammetric Analyzer System controlled by BAS CV-50W software (for PC). The cell used for cyclic voltammetry (CV) contained a glassy-carbon working electrode (BAS standard disk electrode, 3 mm OD), a Pt wire auxiliary electrode (0.5 mm), and a BAS Ag/AgCl (3 M NaCl) reference electrode. Prior to obtaining electrochemical data, solutions were deaerated for at least 30 min with high purity Argon (Ar). Fine polishing of the glassy-carbon working electrode was adapted from the procedure of Keita and co-workers.[37] Unless otherwise noted, scan rates were 10 mV s^{-1}, and all experiments were carried out at ambient temperature under an Ar atmosphere.

For bulk electrolysis and CV of the electrolysis solutions, a BASi Bulk Electrolysis cell was used. The cell was fitted with two working electrodes; one was a glassy-carbon working electrode (BASi MF-2012 standard disk electrode, 3 mm OD) (for CV) and the other (for the electrolysis experiments) was a reticulated vitreous carbon cage (BASi MF-2077). The auxiliary electrode was a platinum wire separated from the bulk electrolyte solution via a fritted compartment, and the reference electrode was Ag/AgCl (BASi MF-2052).

Preparation of Electrolyte Solutions. The aqueous electrolyte solution used for the electrochemical pH study was a constant 0.5 M
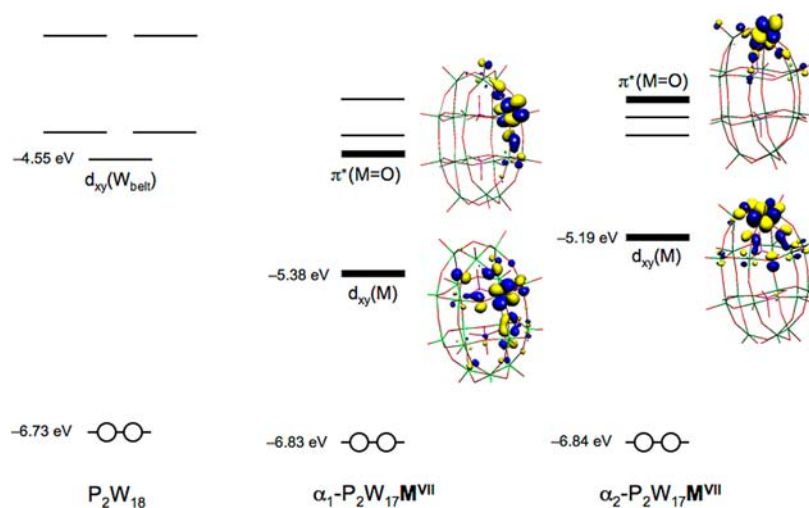
Figure 2. Molecular orbital (MO) representation of the electronic changes observed upon metal substitution from P_2W_{18} to α_1/α_2-$P_2W_{17}Tc^{VII}$. Thick lines represent orbitals of mainly Tc character. Absolute energies of the complexes are in solution.
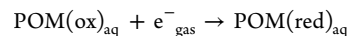
Na_2SO_4 solution prepared at a variety of pH values as described in the Supporting Information.

Assignment of ^{99}Tc and Re Potentials. Electrochemistry experiments were run in replicates yielding identical cyclic voltammo-gram (CV) traces for each compound at each pH. Assignments of the potentials for M^VO-$\alpha1$ and M^VO-$\alpha2$ (M = ^{99}Tc and Re) were made by considering the cyclic voltammograms (CVs) of the complex compared to those of the ligand at each pH. The key to making the assignments is that the W waves of the $\alpha1$ and $\alpha2$ POMs move to more negative potentials with increasing pH. In fact, the second wave for both POMs moves out of the range of the electrochemical experiment as the pH is increased. (Supporting Information, Figures S1, S2) The $M^{VII/VI}$, $M^{VI/V}$, $M^{V/III}$, $M^{V/IV}$, and $M^{IV/III}$ (M = ^{99}Tc, Re) waves remain in the electrochemical window and at higher pH values are well separated from the W waves. Also at all pH values for all complexes, the CVs were deconvoluted to better view the potentials for assignments.
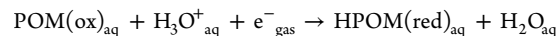
Bulk electrolysis was employed to characterize the number of electrons involved in each redox process. Because of the large volumes of solvent required for bulk electrolysis ($\sim$25 mL), controlled potentiometry experiments could not be conveniently conducted on the samples containing ^{99}Tc. Instead, bulk electrolysis of **ReO**-$\alpha2$ was conducted and compared with an iron containing **FeO**-$\alpha1$ complex at the same concentration where the Fe(III)$\rightarrow$ Fe(II) redox couple involves one electron.[23] The results from these experiments allow us to compare the ^{99}Tc complexes at the same concentration and thus determine the number of electrons involved in each redox process. The bulk electrolysis data for **ReO**-$\alpha2$ (see Supporting Information, Table S1 and description of experiments in the Supporting Information) reflects the assignments of the redox processes associated with one-electron transfers, namely, the Re^{VII}–Re^{VI}, Re^{VI}–Re^{V}, Re^{V}–Re^{IV}, and Re^{IV}–Re^{III} processes.

Computational Details for DFT Treatment. Equilibrium structures and binding energies were obtained using the density functional theory (DFT) as implemented in the ADF 2009.01 program.[38−42] Calculations are characterized by the generalized gradient approximation (GGA), using the Xα model with Becke's corrections[43,44] for exchange, and the VWN parametrization[45] with Perdew's corrections[46,47] for correlation, that is, the BP86 functional. The electrons are described by Slater-type functions. Basis sets are of triple-ζ plus polarization (TZP) quality for all valence electrons, whereas internal or *core* electrons (oxygen: 1s; phosphorus: 1s-2p; technetium: 1s-3d; tungsten, rhenium: 1s-4f) were kept frozen and described by single Slater functions with scalar relativistic corrections via the zeroth-order regular approximation (ZORA), with core potentials generated using the DIRAC program.[38−42] The spin-unrestricted formalism to open shell species was applied.

Given that electrochemical measurements were carried out in aqueous solution, the stabilizing effects of the solvent (water, ε = 78.4) were included in the theoretical treatment of the molecules by means of the *conductor-like screening model* (COSMO).[48−51] The solvent cavity surrounding the anions was created using the solvent-excluding-surface method with fine tesserae. The ionic radii for the atoms that actually define the size of the solvent cavity were chosen to be 1.20 Å for hydrogen, 0.74 Å for metals, and 1.52 Å for oxygen. As has been reported previously, this methodology must be applied to obtain reliable orbital energies and comparable total energies of differently charged anions.[52] For the present case, we calculated the energies for the following process:

$$POM(ox)_{aq} + e^-_{gas} \rightarrow POM(red)_{aq}$$

or

$$POM(ox)_{aq} + H_3O^+_{aq} + e^-_{gas} \rightarrow HPOM(red)_{aq} + H_2O_{aq}$$

where "gas" and "aq" stand for species in gas phase or in aqueous solution, respectively. The free electron is considered as in the gas phase since its energy can be taken as zero.[53]

RESULTS AND DISCUSSION

Comparison of the $\alpha1$ and $\alpha2$ Ligands. *Theoretical Treatment.* The theoretical electronic structure of the parent Wells−Dawson ion, α-$P_2W_{18}O_{62}^{6-}$, has been previously reported[28,29] and, for the purposes of understanding the present study, is shown in Figure 2. The most relevant part of the structure consists of two well separated MO sets; the occupied MO being associated with the oxo ligands and a set of empty MOs of $d_{xy}(W)$ nature, separated by a large energy gap (2.2 eV at the DFT/BP86 level). The first unoccupied metal orbitals are delocalized over the 12 equatorial tungsten atoms located in the belt ($\alpha1$) region[54−58] because the cap $d_{xy}(W)$ orbitals are higher in energy, a fact caused by differences in the local geometry of the cap and belt regions. This means that the first reduction in a Wells−Dawson anion always takes place at the equatorial position,[24,52,55,56] and transition metals sub-stituted into the belt ($\alpha1$) position will be more readily reduced than those substituted in the cap ($\alpha2$).[23,24,56,59]

The optimized geometries for the deprotonated $\alpha1$ and $\alpha2$ isomers give $\Delta E(\alpha_2-\alpha_1) = E(\alpha_2) - E(\alpha_1) = -5.7$ kcal mol^{-1}, which means that the $\alpha2$ isomer is generally more stable than the $\alpha1$. This energy difference is attributed to the different

steric and electronic environments of the vacancy in each isomer. These differences can be explained by the orientation of the internal PO_4^{3-} tetrahedra with respect to the POM vacancy.[22] In $\alpha 1$ one of the internal phosphate oxygens is oriented toward the vacancy and is bound to one W atom. In $\alpha 2$ the phosphate oxygen is not oriented toward the vacancy and is bound to two W atoms making the $\alpha 2$ isomer less nucleophilic than the $\alpha 1$.

Experimental Treatment. Keita, Contant, and Nadjo demonstrated that the $\alpha 1$ and $\alpha 2$ ligands are sensitive to pH and identified decomposition routes.[23,25,59−64] The $\alpha 1$ ligand at pH 3 begins to form the $P_2W_{18}O_{62}^{6-}$ and P_2W_{12} species within hours after dissolution according to cyclic voltammetry.[25] We include our electrochemical characterization of $\alpha 1$ and $\alpha 2$ as a function of pH in the Supporting Information to (1) understand the stabilities of the lacunary anions in our systems and (2) demonstrate their use in making assignments of the Tc and Re redox species (Supporting Information, Figures S1 A, B and Table S2).

To summarize the electrochemical treatment, at pH values of 0.33 and 1 the first W reduction waves for $\alpha 1$ occur at more negative values than those for $\alpha 2$ by −56 mV and −31 mV, respectively. At pH 3 these reduction waves are similar (+5 mV difference) and at pH values of 5 and 7 the first W reduction of $\alpha 1$ is largely pH independent and occurs at more positive potentials than those of $\alpha 2$. These observations indicate that (under these experimental conditions) at pH values below 3, $\alpha 2$ is more easily reduced than $\alpha 1$, while at pH values of 3 and 5, the reduction potentials are similar and at pH 7, the $\alpha 1$ is more easily reduced than $\alpha 2$. The increased nucleophilicity of the $\alpha 1$ ligand is consistent with its ease of reduction compared to the $\alpha 2$ ligand.

Metal Substituted $\alpha 1$ and $\alpha 2$ Complexes. The formal introduction of an M=O unit into either lacunary structure will have a different stabilizing effect on the resulting complex depending on the nature of the metal. To model this theoretically we consider only those orbitals that are involved in the POM redox chemistry, the lowest unoccupied metal-like MOs of $\alpha 1$ and $\alpha 2$. Figure 2 schematically shows the DFT results obtained when a W ion is substituted by Tc in the +7 formal oxidation state (d^0 electron configuration). The LUMO in both of $Tc^{VII}O\text{-}\alpha 1$ and $Tc^{VII}O\text{-}\alpha 2$ is a *pure* d_{xy} orbital localized on the substituting metal atom, with some antibonding interaction from the surrounding bridging oxo sites. These compounds will gain electrons readily because of the low energy of this d orbital; thus the $\alpha 1$ and $\alpha 2$ Wells−Dawson anions containing Tc^{VII} or Re^{VII} are more easily reduced than the structurally similar $\alpha\text{-}[P_2W_{18}O_{62}]^{6-}$ plenary POM. The electrochemistry results, discussed below, are consistent with theory.

Technetium and Rhenium Complexes Electrochemistry. Technetium Complexes. Figures 3 and 5 show the CV data, including the deconvolution data, for the $Tc^VO\text{-}\alpha 1$ and $Tc^VO\text{-}\alpha 2$ compounds, respectively at pH 0 through 7. The voltammograms show the characteristic $\alpha 1$ and $\alpha 2$ Wells−Dawson W redox couples in the negative potential region, as well as redox processes at more positive potentials. On the basis of a comparison to the free $\alpha 1$ and $\alpha 2$ ligands (Supporting Information, Figure S2), and to the bulk electrolysis of the $Fe\text{-}\alpha 1$ and $Re^VO\text{-}\alpha 2$, these redox processes can be assigned (see below). Half-wave potentials ($E_{1/2}$, where $E_{1/2} = (E_c + E_a)/2$) for all redox processes have been summarized in Supporting Information, Table S3 and Table S4, for $Tc^VO\text{-}\alpha 1$ and $Tc^VO\text{-}$

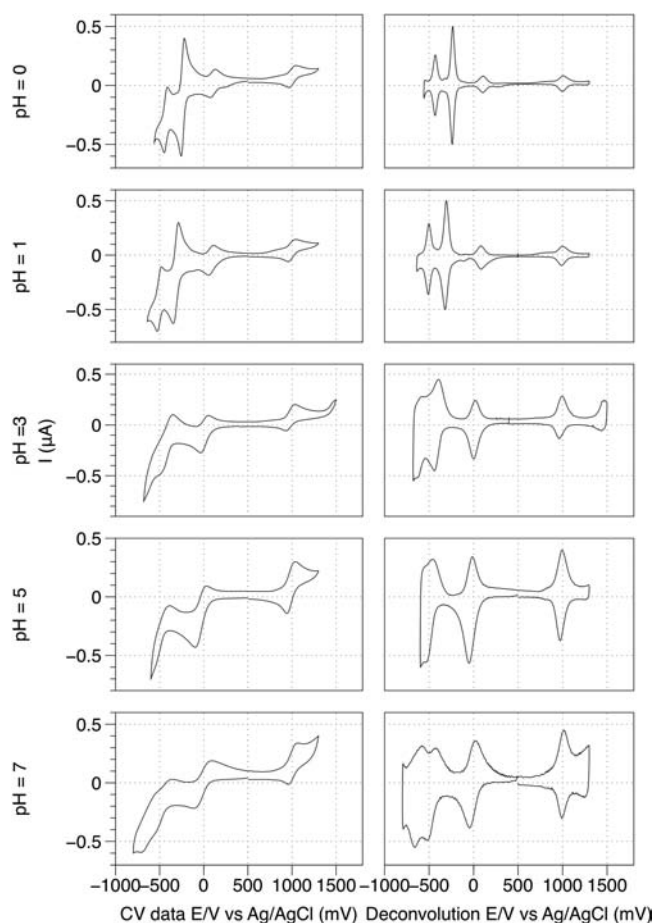**Figure 3.** CV data of 10^{-3} M $K_{7-n}H_n[Tc^VO(\alpha_1\text{-}P_2W_{17}O_{61})]$ as a function of pH. Electrolyte, 0.5 M Na_2SO_4. Working electrode, glassy carbon, auxiliary electrode, platinum wire and reference electrode, Ag/AgCl. Scan rate 10 mV/s.
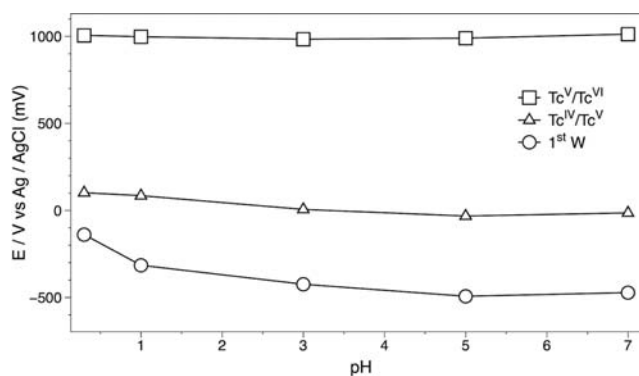

Figure 4. Reduction potentials of 10^{-3} M $[Tc^VO(\alpha_1\text{-}P_2W_{17}O_{61})]^{7-}$ as a function of pH.

$\alpha 2$, respectively. Figures 4 and 6 show plots of the half-wave potentials, as a function of pH, for $Tc^VO\text{-}\alpha 1$ and $Tc^VO\text{-}\alpha 2$, respectively.

The Tc^{VII}/Tc^{VI} couple for both $Tc^VO\text{-}\alpha 1$ and $Tc^VO\text{-}\alpha 2$ compounds is out of the range of the electrochemical window in this solvent system. In some cases, at low pH, we observe an irreversible Tc^{VII}/Tc^{VI} couple that occurs at potentials similar to those for the oxidation of water. This Tc^{VII}/Tc^{VI} couple is illustrated for $Tc^VO\text{-}\alpha 2$ at pH 1 in Supporting Information, Figure S3. However, the Tc^{VII} species is unstable. Prolonged
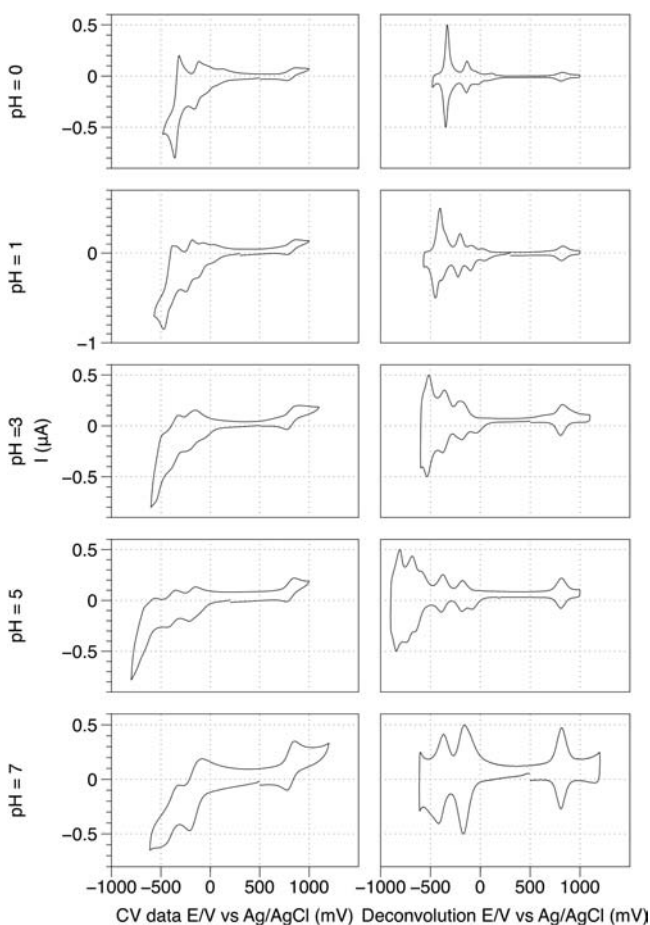
Figure 5. CV data of $K_{7-n}H_n[Tc^VO(\alpha_2-P_2W_{17}O_{61})]$ as a function of pH. Electrolyte, 0.5 M Na_2SO_4. Working electrode, glassy carbon, auxiliary electrode, platinum wire, and reference electrode, Ag/AgCl. Scan rate 10 mV/s.
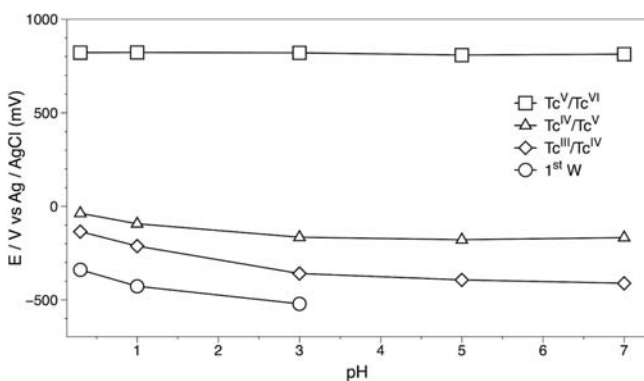

Figure 6. Reduction potentials of 10^{-3} M $[Tc^V(\alpha_2-P_2W_{17}O_{61})]^{7-}$ as a function of pH.

exposure to positive potentials causes dissociation of the complex into a combination of plenary α-$P_2W_{18}O_{62}^{6-}$ and lacunary $P_2W_{17}O_{61}^{10-}$ Wells−Dawson anions and TcO_4^- (as monitored by ^{31}P and ^{99}Tc NMR).

Tc^VO-α1. The two well-resolved (reversible) redox processes at positive potentials, shown in Figure 3, are attributed to two one-electron Tc^V/Tc^{IV} and Tc^{VI}/Tc^V redox processes.[27] Both of these Tc waves are completely reversible over the entire pH range attesting to the stability of the Tc^VO-α1 compound in both highly acidic and slightly basic media.

The $Tc^{V/IV}$ reduction is pH independent or slightly pH dependent (much less than one H$^+$ per one electron reduction process, Supporting Information). The W redox process for Tc^VO-α1 is heavily pH dependent resulting in multiple protons per electron (at least 4H$^+$/2 electrons). The CV data also clearly shows that the $Tc^{V/IV}$ redox process is very well separated from the W waves and is in the positive potential region.

Tc^VO-α2. Figure 5 shows a single well resolved reversible redox process at positive potential that is assigned to the $Tc^{VI/V}$ couple. The characteristic α2 Wells−Dawson W redox couples are observed in the negative potential region as well as two reversible redox couples that occur at more positive potentials than those of the W framework. These couples have been attributed to the 2 successive one-electron Tc^V/Tc^{IV} and Tc^{IV}/Tc^{III} redox processes. While these waves are difficult to discern under highly acidic conditions, they become better resolved as the pH is increased and the W redox waves move to negative potentials that are outside of the electrochemical window.

The W redox couples in the negative potential region show a shift toward more negative potential values with increasing pH. The reduction and oxidation waves for the Tc^{VI}/Tc^V couple are pH independent. On the other hand, Tc $^{V/IV}$, Tc $^{IV/III}$, and the first W reduction processes show pH dependence involving one proton per electron. At pH of about 3, the $Tc^{V/IV}$ and $Tc^{IV/III}$ redox processes become pH independent. This general trend of more negative reduction potentials with increasing pH for the Tc metal center within the α2 ligand means that the reduction of Tc in the α2 vacancy is more easily achieved in an acidic medium.

Tc^VO-α1 and Tc^VO-α2 Comparison. The $Tc^{VI/V}$ redox process is pH independent for Tc^VO-α1 and Tc^VO-α2 suggesting that protonation of the Tc=O is not important for achieving or stabilizing Tc^{VI} and Tc^V in both of the compounds. The $Tc^{VI/V}$ redox process within Tc^VO-α1 is seen to consistently occur at a potential that is on average 180 mV more positive than that of the Tc^VO-α2 compound. The same trend is observed for the $Tc^{V/IV}$ reduction (Table 1). The

Table 1. Comparison of the Half Wave Peak Potentials for $Tc^{V/IV}$ and $Re^{V/IV}$ Reductions in $K_{7-n}H_n[Tc^VO(\alpha_1P_2W_{17}O_{61})]$, $K_{7-n}H_n[Tc^VO(\alpha_2P_2W_{17}O_{61})]$, $K_{7-n}H_n[Re^VO(\alpha_1P_2W_{17}O_{61})]$, and $K_{7-n}H_n[Re^VO(\alpha_2P_2W_{17}O_{61})]$ at pH Values of 0 through 7[a]

$E_{1/2}$ (mV)	pH = 0	pH = 1	pH = 3	pH = 5	pH = 7
α_1-$[Tc^VOP_2W_{17}O_{61}]^{7-}$	+102	+81	+6	−32	−14
α_2-$[Tc^VOP_2W_{17}O_{61}]^{7-}$	−37	−93	−165	−178	−164
$\Delta(\alpha_1-\alpha_2)$	+139	+174	+159	+146	+141
α_1-$[Re^VOP_2W_{17}O_{61}]^{7-}$	−205[b]	−250[b]	−283	−274	−287
α_2-$[Re^VOP_2W_{17}O_{61}]^{7-}$	−230[b]	−263[b]	−271	−263	−262
$\Delta(\alpha_1-\alpha_2)$	+25	+13	−12	−11	−25

[a]Scan rate 10 mV s^{-1}. [b]Reported values are of the $Re^{V/III}$ reduction.

$Tc^{V/IV}$ reduction in Tc^VO-α1 is only slightly pH dependent whereas the $Tc^{V/IV}$ reduction in Tc^VO-α2 shows one proton consumed for the one electron reduction process until pH 3. At all pH values (0 through 7) the $Tc^{V/IV}$ redox couple in Tc^VO-α1 occurs at a more positive potential of ~150 mV compared to the $Tc^{V/IV}$ redox couple in Tc^VO-α2. This phenomenon is consistent with observations that transition metals substituted

into the belt ($\alpha1$) position will be more readily reduced than those substituted in the cap ($\alpha2$).[23,24,56,59]

Free energy calculations for the $Tc^V + 1e^- \rightarrow Tc^{IV}$ process (Supporting Information, Table S5) track with the potentials for the Tc^V/Tc^{IV} process and show that the free energy requirement associated with the reduction of Tc in the **Tc^VO-$\alpha2$** complex is greater than that for the **Tc^VO-$\alpha1$** (by an average of 12.2 kJ) at all pH values.

Rhenium Complexes. Figures 7 and 9 present the CV and deconvolution data for **Re^VO-$\alpha1$** and **Re^VO-$\alpha2$**, respectively, at
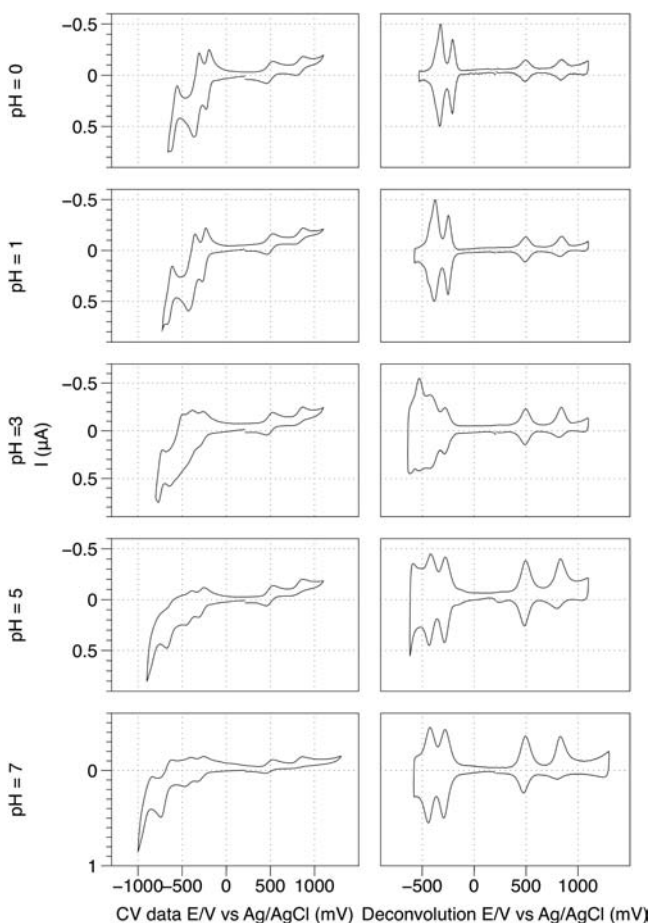
Figure 7. CV data of 10^{-3} M $K_{7-n}H_n[Re^VO(\alpha_1\text{-}P_2W_{17}O_{61})]$ as a function of pH. Electrolyte, 0.5 M Na_2SO_4. Working electrode, glassy carbon, auxiliary electrode, platinum wire, and reference electrode, Ag/AgCl. Scan rate 10 mV/s.

pH values from 0 to 7. The comparison of **Re^VO-$\alpha1$** and **Re^VO-$\alpha2$** to the $\alpha1$ and $\alpha2$ ligands is presented in Supporting Information, Figure S4. Half-wave potentials are summarized in Supporting Information, Tables S6 and S7 for **Re^VO-$\alpha1$ and Re^VO-$\alpha2$**, respectively. A plot of the half-wave potentials as a function of pH is shown in Figure 8 and Figure 10 for **Re^VO-$\alpha1$** and **Re^VO-$\alpha2$**, respectively.

Re^VO-$\alpha1$. The quasi-reversible pH independent wave at +839 mV is attributed to Re^{VII}/Re^{VI} redox process, and the reversible wave centered at $E_{1/2}$ = +490 is attributed to the Re^{VI}/Re^V redox process.[65] Both redox processes are pH independent.

In the negative potential region, two reversible redox couples are assigned to a 2 electron Re^V/Re^{III} and tungsten redox processes. The couple attributed to the Re^V/Re^{III} redox process
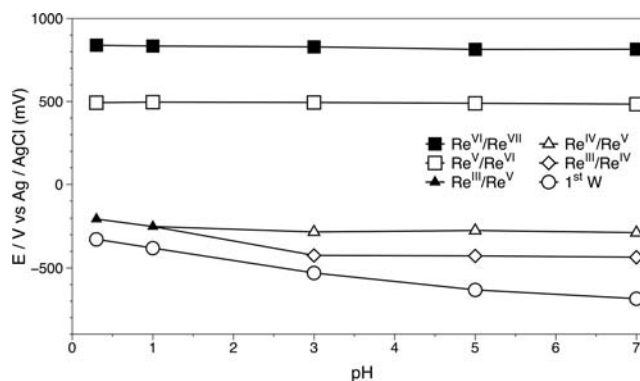
Figure 8. Reduction potentials of 10^{-3} M $[Re^VO(\alpha_1\text{-}P_2W_{17}O_{61})]^{7-}$ as a function of pH.
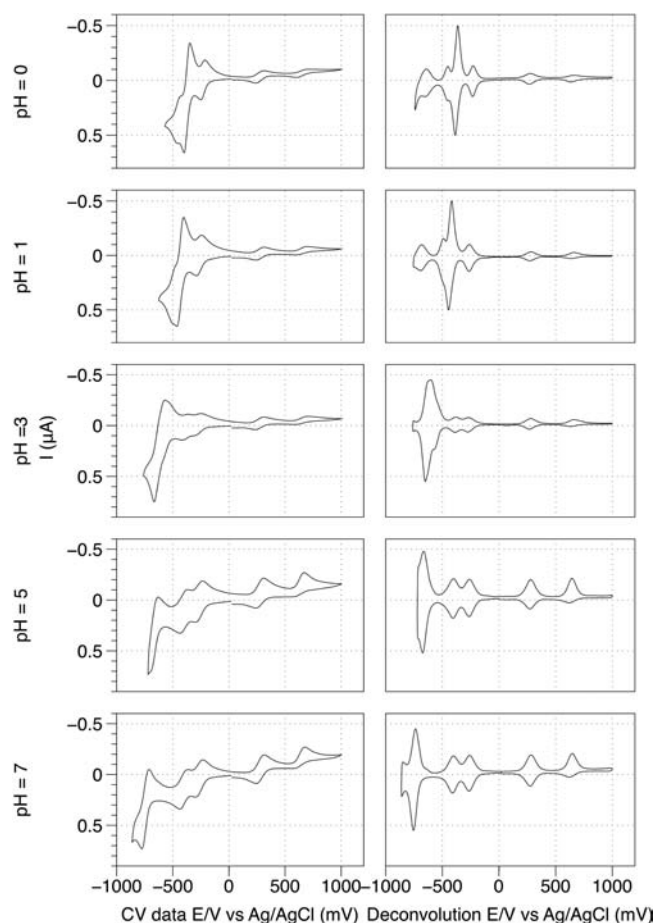
Figure 9. CV data of 10^{-3} M $K_{7-n}H_n[Re^VO(\alpha_2\text{-}P_2W_{17}O_{61})]$ as a function of pH. Electrolyte, 0.5 M Na_2SO_4. Working electrode, glassy carbon, auxiliary electrode, platinum wire, and reference electrode, Ag/AgCl. Scan rate 10 mV/s.

shows a shift toward more negative potential with increasing pH up to pH 3, and the pH dependence suggests that one proton is involved per one electron. Above pH 3, the wave is seen to split into two one electron processes (Re^V/Re^{IV} and Re^{IV}/Re^{III}) that are pH independent. There is an observable increase in the splitting between the Re^{IV}/Re^{III} and W-framework$^{VI/V}$ redox couples with increasing pH.

Re^VO-$\alpha2$. The well-resolved redox processes in the positive potential region are attributed to the two one-electron quasi-reversible Re^{VII}/Re^{VI} (+645 mV) and fully reversible Re^{VI}/Re^V
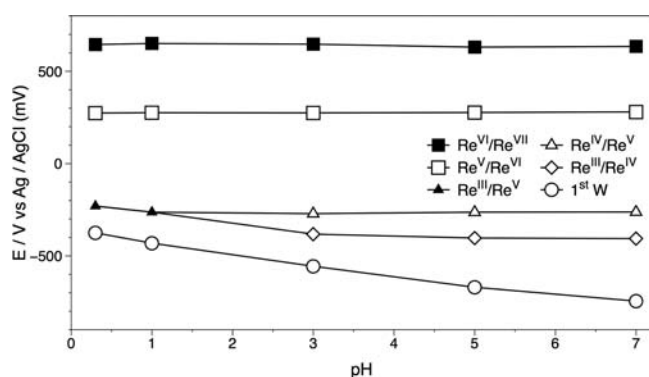
Figure 10. Reduction potentials of 10^{-3} M $[Re^VO(\alpha_2\text{-}P_2W_{17}O_{61})]^{7-}$ as a function of pH.

(+274 mV) redox processes The half-wave potentials for the Re^{VI}/Re^V and Re^{VII}/Re^{VI} redox processes are pH independent over the entire pH range.

In the negative potential region, two redox processes are observed. These are assigned to the 2 electron $Re^{V/III}$ where the pH dependence suggests that 2 protons accompany the 2 electron reduction and a W redox process. At pH > 1, the two electron wave splits into two one electron reductions that are assigned to the $Re^{IV/III}$ and $Re^{V/IV}$ processes. Above pH 1, the $Re^{V/IV}$ redox process is pH independent while the $Re^{IV/III}$ and W redox processes shift toward more negative potential values. The pH dependence of the $Re^{IV/III}$ reduction between pH 0−3 shows that this process consumes 1 proton per electron. These redox processes are consistent with the work of Ortega and Pope[65] for $[Re^VO(SiW_{11}O_{39})]^{5-}$, where Re^VO is bound into the $\alpha\text{-}SiW_{11}O_{39}{}^{8-}$ lacunary Keggin ion. The general shift of the $Re^{IV/III}$ and $Re^{V/IV}$ reduction couples toward more negative reduction potentials with increasing pH is consistent with observations for Tc; reduction of Re^V and Re^{IV} in the $\alpha2$ vacancy is more easily achieved in an acidic medium.

$Re^VO\text{-}\alpha1$ and $Re^VO\text{-}\alpha2$ Comparison. The $Re^{VII/VI}$ and $Re^{VI/V}$ redox processes within **$Re^VO\text{-}\alpha1$** occur at potentials that are, on average, 184 mV and 215 mV, respectively, more positive than that of the **$Re^VO\text{-}\alpha2$** compound, consistent with the facile reduction in the $\alpha1$ vacancy compared to the $\alpha2$ vacancy. The $Re^{VII/VI}$ wave remains quasi-reversible at all pH values which speaks to the low redox stability of Re^{VII} within the POM frameworks. In fact, exposure of both **$Re^VO\text{-}\alpha1$** and **$Re^VO\text{-}\alpha2$** to oxidizing potentials (>830 mV) leads to irreversible decomposition of the complexes to the lacunary Wells−Dawson anions and $ReO_4{}^-$ as observed by CV. On the other hand, the **$Re^{VII}O\text{-}\alpha2$** as a TBA salt is stable in acetonitrile and has been isolated and characterized.[36]

The pH independence of the $Re^{VII/VI}$ and $Re^{VI/V}$ for both **$Re^VO\text{-}\alpha1$** and **$Re^VO\text{-}\alpha2$** suggests that protonation of the Re= O is not important for achieving and stabilizing the Re^{VII}, Re^{VI}, and Re^V oxidation states. At pH 0 and 1, both **$Re^VO\text{-}\alpha1$** and **$Re^VO\text{-}\alpha2$** show one two-electron process that is attributed to $Re^{V/III}$. At pH ≥ 1, this wave splits into two one electron processes. Free energy calculations (Supporting Information, Table S8) in the pH range 3−7 track with the potentials and demonstrate that ΔG for **$Re^VO\text{-}\alpha1$** is only marginally greater than that of **$Re^VO\text{-}\alpha2$** (by an average of 1.5 kJ). Examination of Table 1 shows that the reduction potentials assigned as $Re^{V/IV}$ couples for **$Re^VO\text{-}\alpha1$** and **$Re^VO\text{-}\alpha2$** are very similar.

Comparison between $Tc^VO\text{-}\alpha1/\alpha2$ and $Re^VO\text{-}\alpha1/\alpha2$. Although Tc^V and Re^V have the same d^2 outer shell configuration when substituted into the $\alpha1$ and $\alpha2$ POM frameworks, there are fundamental differences between the two elements from both an experimental and a theoretical perspective. Table 2 compares the CV data for the redox waves of the Tc and Re complexes of $\alpha1$ and $\alpha2$ over the entire pH range. The $Re^{VII/VI}$ redox couple is observed for both the $\alpha1$ and $\alpha2$ complexes but not for the Tc analogues within this aqueous electrochemical window. This phenomenon is consistent with the chemistry of Tc and Re, where Re complexes tend toward their high oxidation states while the Tc analogues tend toward more stable reduced states.[30−33] To summarize, in all cases, Tc is more easily reduced than the Re counterpart.

$Tc^VO\text{-}\alpha1$ and $Re^VO\text{-}\alpha1$. The Tc^{VI} reduction to Tc^V occurs consistently at a potential that is 500 mV more positive than that of the corresponding Re^{VI}. The $Tc^V \rightarrow Tc^{IV}$ reduction process is on the order of 273−300 mV more positive compared to the Re analogue. This is consistent with periodic trends.

$Tc^VO\text{-}\alpha2$ and $Re^VO\text{-}\alpha2$. The Tc^{VI}/Tc^V redox process occurs at a potential that is, on average, +540 mV more positive than that of the Re^{VI}/Re^V. In the **$Tc^VO\text{-}\alpha2$** species, both the $Tc^{V/IV}$ and the $Tc^{IV/III}$ are separated over the entire pH range. In comparison, the **$Re^VO\text{-}\alpha2$** shows a combined 2 electron $Re^{V/III}$ reduction at pH 0 and 1, and from pH 3 to 7, separate $Re^{V/IV}$ and $Re^{IV/III}$ processes similar to the $[Re^VO(SiW_{11}O_{39})]^{5-}$.[65] For both the $M^{V/IV}$ and $M^{IV/III}$ reductions the **$Tc^VO\text{-}\alpha2$** is more easily reduced compared to **$Re^VO\text{-}\alpha2$**, with larger differences under acidic conditions.

HOMO−LUMO Frontier Orbitals Trends. A graphical depiction of the highest occupied MOs (HOMOs) and LUMOs extracted from the electrochemistry data for both $M^VO\text{-}\alpha1$ and $M^VO\text{-}\alpha2$ (M = ^{99}Tc and Re) at pH 1 is presented in Figure 11. This graphical presentation can be qualitatively compared to the MOs obtained from the DFT calculations,

Table 2. Comparison of the Differences in Potential for the Redox Processes of Tc and Re Complexes of $\alpha_1P_2W_{17}O_{61}{}^{10-}$ and Tc and Re Complexes of $\alpha_2P_2W_{17}O_{61}{}^{10-}$

	$E_{1/2}$Tc α_1 − $E_{1/2}$Re α_1			$E_{1/2}$Tc α_2 − $E_{1/2}$Re α_2			
pH	W (1st wave) $\Delta E_{1/2}$ (mV)	$M^{IV/V}$ $\Delta E_{1/2}$ (mV)	$M^{V/VI}$ $\Delta E_{1/2}$ (mV)	W (1st wave) $\Delta E_{1/2}$ (mV)	$M^{III/IV}$ $\Delta E_{1/2}$ (mV)	$M^{IV/V}$ $\Delta E_{1/2}$ (mV)	$M^{V/VI}$ $\Delta E_{1/2}$ (mV)
0	+231	+307	+513	+36		+193	+548
1	+118	+335	+502	+4	+51	+170	+547
3	+106	+289	+490	+35	+23	+106	+546
5		+242	+501		+10	+85	+532
7		+273	+529		−5	+98	+531

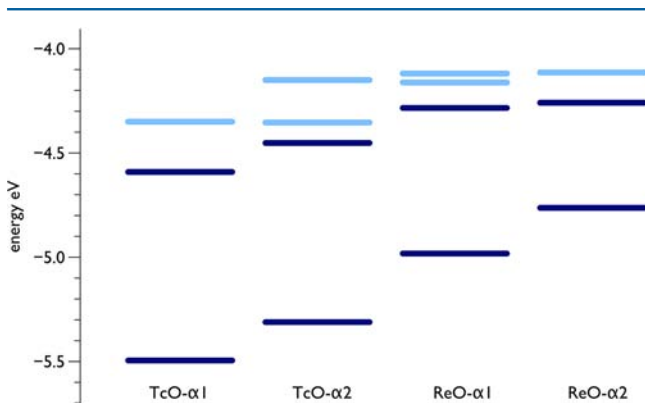discussed below. The HOMO−LUMO gap energies are presented in Table 3.

Figure 11. Graphical comparison of the HOMO−LUMO gap extracted from electrochemistry experiments at pH 1 for $K_{7-n}H_n[Tc^VO(\alpha_1\text{-}P_2W_{17}O_{61})]$, $K_{7-n}H_n[Tc^VO(\alpha_2\text{-}P_2W_{17}O_{61})]$, $K_{7-n}H_n[Re^VO(\alpha_1\text{-}P_2W_{17}O_{61})]$, and $K_{7-n}H_n[Re^VO(\alpha_2\text{-}P_2W_{17}O_{61})]$. The dark blue lines represent the HOMO and LUMO and the light blue lines represent the nearest W redox processes.

Table 3. HOMO−LUMO Energy Gap Values for $[Tc^VO(\alpha_1\text{-}P_2W_{17}O_{61})]^{7-}$, $[Tc^VO(\alpha_2\text{-}P_2W_{17}O_{61})]^{7-}$, $[Re^VO(\alpha_1\text{-}P_2W_{17}O_{61})]^{7-}$, and $[Re^VO(\alpha_2\text{-}P_2W_{17}O_{61})]^{7-}$

pH	α_1-$[Tc^VOP_2W_{17}O_{61}]^{7-}$ (eV)	α_2-$[Tc^VOP_2W_{17}O_{61}]^{7-}$ (eV)	Δ $(\alpha_1 - \alpha_2)$ (eV)
0	0.898	0.853	0.045
1	0.911	0.910	0.0015
3	0.968	0.988	0.02
5	1.015	0.971	0.034
7	1.021	0.971	0.05

pH	α_1-$[Re^VOP_2W_{17}O_{61}]^{7-}$ (eV)	α_2-$[Re^VOP_2W_{17}O_{61}]^{7-}$ (eV)	Δ $(\alpha_1 - \alpha_2)$ (eV)
0	0.692	0.500	0.192
1	0.740	0.535	0.157
3	0.771	0.542	0.151
5	0.757	0.535	0.157
7	0.765	0.537	0.155

In POMs, the filled oxygen orbitals comprise the lowest MOs and the unfilled tungsten orbitals mostly comprise the higher unfilled MOs. In transition metal substituted POMs, the "frontier orbitals" are mostly composed of the transition metal d orbitals with possible overlap with W-based orbitals. In this case, the electrochemical cyclic voltammetry data gives an accurate assessment of the frontier orbitals, that is, the HOMO and the LUMO. The HOMO−LUMO energy gap can be extracted from electrochemical data by calculating the difference between the oxidation peak potential (Ea) in the CV of the $Tc^{VI/V}$ couple (HOMO) and the reductive peak potential

(Ec) of the $Tc^{V/IV}$ couple (LUMO). These values are relative to the normal energy of 4.28 eV.[53,66]

The LUMO for **Tc^VO-$\alpha1$** is well separated from the W bands. In the case of the **Re^VO-$\alpha1$** and **Tc/Re^VO-$\alpha2$** complexes, the W bands are very close to the LUMO energies and, in fact, may overlap at low pH. The overlap/mixing of M and W orbitals would be greater for the Re complexes since the valence d orbitals are higher in energy compared to Tc. These experimental data track very well with the theoretical treatment (vide infra) where the LUMO (π^* Tc=O) for **Tc^VO-$\alpha1$** is well separated from the higher energy W bands. The theoretical data show that the LUMOs for the **Re^VO-$\alpha1$** and **Tc/Re^VO-$\alpha2$** complexes are W-based with the π^* Tc/Re=O orbital at slightly higher energies. It is clear from Figure 11, that the potentials, and thus energies, are very close for the **Re^VO-$\alpha1$** and **Tc/Re^VO-$\alpha2$** complexes. The DFT calculations, discussed below, also predict the lowering of the π^* Tc/Re=O orbitals upon protonation that is also consistent with experimental observations (Supporting Information, Figures S5 and S6).

The HOMO−LUMO energy gaps determined from electrochemistry experiments (calculated in electron volts (eV)) for **Tc^VO-$\alpha1$**, **Tc^VO-$\alpha2$**, and **Re^VO-$\alpha1$** and **Re^VO-$\alpha2$** over the pH range are presented in Table 3. The salient points are that the Tc species experience significantly larger energy gaps than the Re complexes, for protonated and nonprotonated conditions. The HOMO−LUMO energy gaps are similar in the **Tc^VO-$\alpha1$** and **Tc^VO-$\alpha2$** complexes. However, the energy gaps for **Re^VO-$\alpha2$** are significantly lower than those for **Re^VO-$\alpha1$** by about 150−190 meV.

The significantly smaller HOMO−LUMO gap in the Re complexes and specifically in the **Re^VO-$\alpha2$** complex may speak to the "softness" of the Re complexes compared to the Tc complexes using the Hard−Soft Acid Base vernacular. Considering Table 1 and Table 3, the $Re^{V/IV}$ reduction of **Re^VO-$\alpha2$** is comparable to that of the **Re^VO-$\alpha1$** compound. In fact, the $Re^{V/IV}$ reduction of **Re^VO-$\alpha2$** is more positive than that of the **Re^VO-$\alpha1$** compound at pH $\geq$ 3.

DFT Discussion. The energy differences between the two isomers (**$M^{VII}O$-$\alpha1$** and **$M^{VII}O$-$\alpha2$**) were computed (as $\Delta E = E(\alpha_2) - E(\alpha_1)$) to be −4.8 and −3.5 kcal mol^{-1} for Tc and Re respectively. This means that for both Tc^{VII} and Re^{VII} the metal substituted $\alpha2$ complex is more stable than that of the $\alpha1$. The nucleophilicity of the $\alpha1$ and $\alpha2$ vacancies do not have as much influence on the energy differences, $\Delta E(\alpha_2-\alpha_1)$, in the metal complexes as compared to the lacunary POMs.

Reduction energies (REs) were computed for both Tc and Re (in oxidation states VII, VI, and V) substituted into the $\alpha1$ and $\alpha2$ POMs and are summarized in Table 4. The $Tc^{VII/VI}$ process gives very negative REs of −5.41 and −5.18 eV for the $\alpha1$ and $\alpha2$ isomers, respectively, reinforcing the idea that **$Tc^{VII}O$-$\alpha1$** and **$Tc^{VII}O$-$\alpha2$** are too easily reduced to be stable. Experimentally, Tc^V can be reversibly oxidized to Tc^{VI} (a reversible $Tc^{VI/V}$ redox process is observable in the CV data), but oxidation to Tc^{VII} results in decomposition (vide supra).

Table 4. Reduction Energies^a of the Nonprotonated α_1- and α_2-$P_2W_{17}M$ Species (M = Tc, Re)

	Tc			Re		
reduction process	α_1	α_2	$\Delta RE(\alpha_2-\alpha_1)$	α_1	α_2	$\Delta RE(\alpha_2-\alpha_1)$
VII/VI^b	−5.41	−5.18	0.23	−4.91	−4.62	0.29
VI/V	−4.92	−4.74	0.18	−4.62	−4.38	0.24

^{a}Values in eV. ^{b}This process does not take place in Tc derivatives.

The REs for the Re$^{VII/VI}$ processes are −4.91 eV for **α1** and −4.62 eV for **α2**, so the trend is equivalent to that observed for Tc, but at ∼0.5 eV less negative values. This is consistent with the more diffuse character of the d orbitals of Re which lead to LUMOs of higher energy as observed in the analysis of CV data, vide supra. Moreover, experimentally, the Re$^{VII/VI}$ redox couples are "quasi- reversible" which is consistent with the theoretical treatment.

After the first reduction (i.e., M^{VII} →M^{VI}), **Tc^{VI}O-α1** and **Tc^{VI}O-α2** show very similar energies, $\Delta E(\alpha_2-\alpha_1) = 0.5$ kcal mol^{-1}, whereas **Re^{VI}O-α1** is 3.3 kcal mol^{-1} more stable than **Re^{VI}O-α2**. The second reduction for Tc (VI → V) gives RE = −4.92 and −4.74 eV for **α1** and **α2** indicating that the reduction of the metal is still more favorable when it is substituted into the **α1** vacancy (Supporting Information, Table S9); this is consistent with experimental results.

In general the favorable reduction of either Tc or Re substituted into **α1** is reasonable considering the orbital energies depicted in Figure 2. When a metal (M^{VII}) is substituted into the lacunary POMs the resulting empty metal orbitals are at lower energy than those of the W. Favorable reduction of Tc over Re is observed because of the low lying Tc LUMOs compared to those of Re. After the second reduction, **Tc^{V}O-α1** becomes the most stable isomer (by 4.7 kcal mol^{-1}). This stability also occurs in the Re derivative with 8.8 kcal mol^{-1} in favor of **Re^{V}O-α1**.

These structures show small and very localized geometrical changes as you move from M^{VII} to M^{V}. In the case of Tc, only the Tc−O−W bridging oxygens elongate by 0.1 Å since the formally nonbonding d$_{xy}$(Tc) is occupied. At this point, the Tc≡O$_{term}$ distance has not changed appreciably. Considering Tc chemistry, this is quite consistent. The Tc≡O$_{term}$ bond should be reasonably strong and short, and we have observed this in the extended X-ray absorption fine structure (EXAFS) data for **Tc^{V}O-α1** and **Tc^{V}O-α2**.[27]

Understanding the next reduction step (M^{V} → M^{IV}) is less intuitive. Figure 12 shows the sequence of MOs for **Tc^{V}O-α1/-α2** and **Re^{V}O-α1/-α2** determined by DFT calculations. From the DFT calculations, the **Tc^{V}O-α1** is the only species where the LUMO is technetium based (π^*(Tc≡O)). This tracks well

with the experimental data where the Tc$^{V/IV}$ redox process is at such positive potential for **Tc^{V}O-α1** compared to **Tc^{V}O-α2** and **Re^{V}O-α1/-α2** and is well separated from the W bands. DFT calculations suggest that the reduction would take place preferentially in the W centers for **Tc^{V}O-α2** and **Re^{V}O-α1/-α2** particularly for Re-based compounds which present π^*(Re≡O) orbitals at rather high energies, as shown in Figure 12.

To bring the DFT calculations and the experimental electrochemistry into accord, the M$^{V/IV}$ reduction process for **Tc^{V}O-α2** and **Re^{V}O-α1/-α2** must involve protonation. DFT results indicate that the Re$^{V/IV}$ reduction process requires protonation on the terminal Re≡O oxygen, a possibility already documented by Pope and co-workers for acidic and neutral conditions.[65] Without protonation, the one-electron reduction of **Re^{V}O-α1** gives **Re^{V}O-α1_1e**, that is, an extra electron delocalized over some of the W atoms and not localized on the Re center. The W waves and Re waves are very close to each other so it is potentially possible that the reductions can be associated with the W centers. However, it is likely that the Re centers are reduced if protonation of the Re≡O terminal oxygen takes place,[65] which permits the stabilization of the π^* antibonding orbital and would set up a favorable distorted octahedral ligand field environment for the Re(IV) (d^3) oxidation state (see Figure 13). The stabilization of
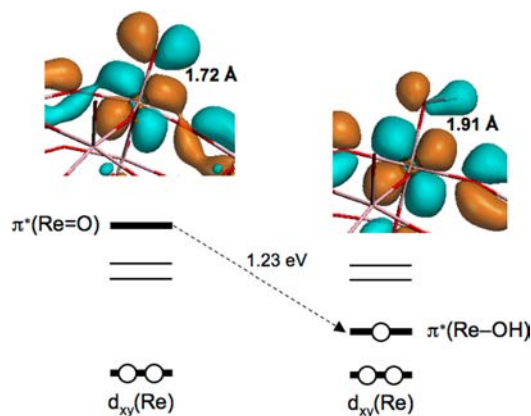
Figure 13. Evolution of the MOs upon reduction plus protonation at the terminal oxygen site Re≡O of [Re^{V}O(α_1-P$_2$W$_{17}$O$_{61}$)]$^{7-}$. The Re−O distances in both states are shown as well as the π^*(Re−O) orbital involved in the reduction process.

the π^* antibonding orbital upon *reduction* plus *protonation* was computed to be 1.1 eV for Tc, and 1.2 eV for Re compounds. This orbital is then lower in energy than the first unoccupied W-like MO. Protonation at any other plausible site does not entail so much energy change of an orbital and can by no means favor Re^{IV}. The atomic spin populations calculated for the **Re^{IV}O-α1** and **Tc^{IV}O-α1** complexes are 0.92 and 0.94, respectively, indicating that the third metallic electron is fully localized.

Insight into the Electronic Environments of the α1 and α2 Defects. The theory and experiment, including pH dependence for the M$^{V/IV}$ (M = ^{99}Tc and Re) redox couples, along with previously described XAS of the **Tc^{V}O-α1** and **Tc^{V}O-α2**[27] together provide insight into the differences in the
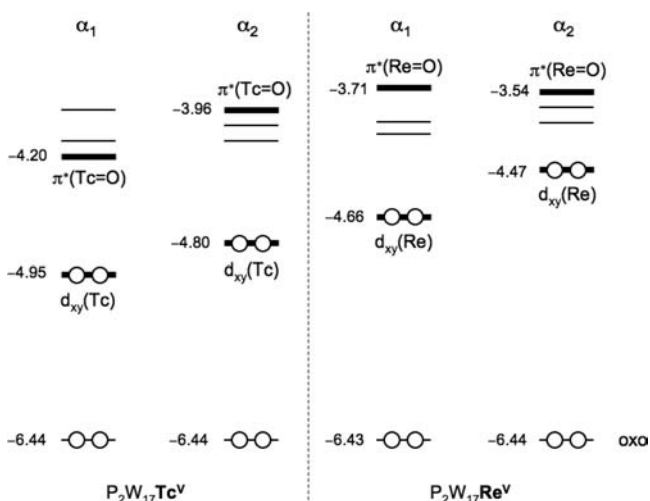

Figure 12. Sequence of the doubly occupied highest occupied and the first unoccupied metal-like MOs for the *nonprotonated* α_1/α_2-[M^{V}O(P$_2$W$_{17}$O$_{61}$)]$^{7-}$ (M = Tc and Re) species. Energies are in eV. Thick lines represent orbitals of mainly Tc (respectively Re) character.

electronic environments provided by the $\alpha1$ and $\alpha2$ defects. The $Tc^{V/IV}$ redox couple for Tc^VO-$\alpha1$ shows no or little pH dependence compared to the Tc^VO-$\alpha2$ analogue that shows a one proton per electron dependence from pH 0 to 3 and is pH independent above 3. Additionally, the first W couple for Tc^VO-$\alpha1$ is heavily pH dependent resulting in multiple protons per electron compared to the first W couples in the other species that show one proton per one electron transfer.

Previous EXAFS and X-ray absorption near edge structure (XANES) studies of the Tc^VO-$\alpha1$ and Tc^VO-$\alpha2$[27] revealed significant structural differences that are likely the cause for the disparity in the electrochemical reduction behavior. The structure for Tc^VO-$\alpha2$ is consistent with a square pyramidal environment for Tc(V). The oxygen coordination environment contains a very short terminal Tc^V=O bond, 4 Tc−O single bonds, and a long Tc---O(phosphate) interaction. On the other hand, the EXAFS data for the Tc^VO-$\alpha1$ suggest that the Tc(V) center has been "pulled into" the Wells−Dawson ion relative to the position of the belt W atom. The data show the short Tc^V=O bond but 5 Tc−O single bonds without the long Tc−O interaction and show W,P distances that are shorter than expected. These data are consistent with the formation of a dative metal−metal bond between Tc(V) and the nearest tungsten atom in the $\alpha1$ lacunary POM. This structure is likely a consequence of the highly basic oxygen positioned in the $\alpha1$ defect compared to the lower basicity oxygen atoms in the $\alpha2$ defect.[22,24−26,59−61] [183]W NMR data are consistent with this structural assignment. The [183]W NMR of Re^VO-$\alpha1$ suggests a similar structure.

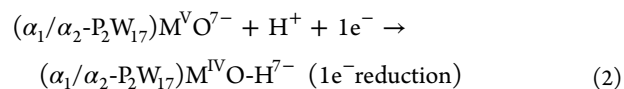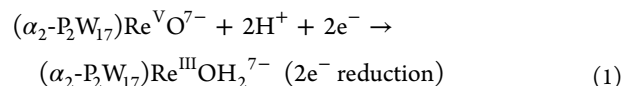The more facile reduction of Tc^VO-$\alpha1$ and pH independence (or slight pH dependence) of the $Tc^{V/IV}$ reduction process relative to Tc^VO-$\alpha2$ may be due to the Tc−W interaction in Tc^VO-$\alpha1$, which should stabilize the lower Tc oxidation states. The Tc−W interaction in this structure renders the Tc in Tc^VO-$\alpha1$ somewhat less electron rich relative to Tc^VO-$\alpha2$ as determined by the XANES data.[27] Because of the nature of the structure and the less electron rich Tc, the Tc^VO-$\alpha1$ does not require protons to facilitate the $Tc^{V/IV}$ reduction. While the Re analogue may have the same or similar structure (based on a similar [183]W NMR[27]), the inherent difficulty to reduce Re compared to Tc may result in the need for protonation to facilitate $Re^{V/IV}$ reduction in Re^VO-$\alpha1$. It is clear that the electron transfer properties between the $\alpha1$ and $\alpha2$ sites are unmistakably different. This highlights the inequivalency of the two sites, and their impact on the chemical properties of transition metal cations substituted in these positions.

Chemistry of Tc(IV) and Re(IV) and Mechanistic Considerations.

The theoretical treatment and experimental data are fully consistent with the chemistry of Tc(IV) and Re(IV), in general and specifically with our observations of Tc(IV) in $\alpha1$ and $\alpha2$ sites. First, Tc(IV) and Re(IV) complexes generally exhibit distorted octahedral coordination geometry with the three d electrons occupying the t_{2g} orbital set resulting in paramagnetic complexes with only Tc−O or Re−O single bonds. Protonation of the terminal Tc=O upon addition of electron(s) to form weaker, longer Tc−O single bonds is consistent with the observed chemistry of Tc(IV).[67]

We observe formation of Tc(IV)-O species frequently in the synthesis of Tc^V $\alpha1$/-$\alpha2$ complexes. These have been found in traditional synthesis[27,68] as well as via "non-traditional" routes such as photoactivated reduction of TcO_4^- by $\alpha2$, in the presence of a sacrificial electron donor, to form a Tc(IV) $\alpha2$ "intermediate".[21] The formation of a stable Tc(IV) "inter-
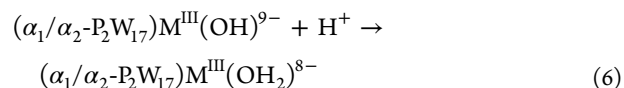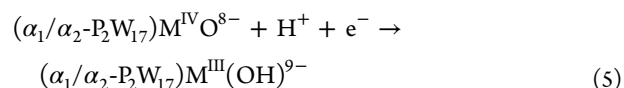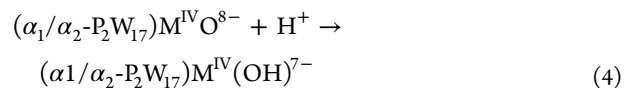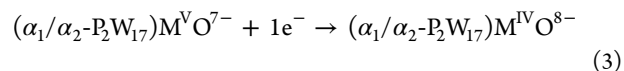
mediate" without formation of TcO_2 is remarkable and attests to the stability of this Tc(IV) $\alpha2$ entity. Moreover, this observation is consistent with the reversible or quasi-reversible $Tc^{V/IV}$ couple in this study with respect to both Tc^VO-$\alpha1$ and Tc^VO-$\alpha2$.

Under low pH conditions where the redox processes (for Tc^VO-$\alpha2$ and Re^VO-$\alpha1$/-$\alpha2$) are acid dependent, the plausible mechanisms for one and two electron (Re^VO-$\alpha2$) reductions are similar to those submitted by Ortega and Pope:[65]

$$(\alpha_2\text{-}P_2W_{17})Re^VO^{7-} + 2H^+ + 2e^- \rightarrow$$
$$(\alpha_2\text{-}P_2W_{17})Re^{III}OH_2{}^{7-} \ (2e^- \text{ reduction}) \quad (1)$$

$$(\alpha_1/\alpha_2\text{-}P_2W_{17})M^VO^{7-} + H^+ + 1e^- \rightarrow$$
$$(\alpha_1/\alpha_2\text{-}P_2W_{17})M^{IV}O\text{-}H^{7-} \ (1e^-\text{reduction}) \quad (2)$$

In reactions 1 and 2 (α_1, M = Re; α_2, M = [99]Tc, Re), protons facilitate the addition of electrons to the antibonding π^* (M=O) orbital resulting in formation of the M^{III}−OH_2 (2 electron process) or M^{IV}−OH (one electron process). Equations 1 and 2 are consistent with the number of protons consumed per electron for the respective processes (Supporting Information).

In the pH independent region, the addition of an electron to the antibonding $\pi(M=O)^*$ (M = Tc,Re) orbitals will result in a weakening (and lengthening) of the M-O bond. The M-O oxygen atom will then be susceptible to protonation. Plausible mechanisms include:

$$(\alpha_1/\alpha_2\text{-}P_2W_{17})M^VO^{7-} + 1e^- \rightarrow (\alpha_1/\alpha_2\text{-}P_2W_{17})M^{IV}O^{8-}$$
$$(3)$$

$$(\alpha_1/\alpha_2\text{-}P_2W_{17})M^{IV}O^{8-} + H^+ \rightarrow$$
$$(\alpha1/\alpha_2\text{-}P_2W_{17})M^{IV}(OH)^{7-} \quad (4)$$

$$(\alpha_1/\alpha_2\text{-}P_2W_{17})M^{IV}O^{8-} + H^+ + e^- \rightarrow$$
$$(\alpha_1/\alpha_2\text{-}P_2W_{17})M^{III}(OH)^{9-} \quad (5)$$

$$(\alpha_1/\alpha_2\text{-}P_2W_{17})M^{III}(OH)^{9-} + H^+ \rightarrow$$
$$(\alpha_1/\alpha_2\text{-}P_2W_{17})M^{III}(OH_2)^{8-} \quad (6)$$

Comment on Future Work. These redox active metals and redox active ligands are complicated systems. Although the rhenium and tungsten redox waves are observed to overlap in the negative region of the CV at low pH, we are confident in our assignments because (1) the W waves move to more negative potentials with increasing pH, revealing the Tc and Re redox waves, (2) this work is consistent with the reports by Pope and Ortega for the Re Keggin systems,[65] and (3) the data is consistent for d^3 systems. Despite this, we acknowledge the need to unambiguously confirm these assignments with additional computational and experimental studies.

Spectroelectrochemistry (using EXAFS and XANES) is a very useful technique to reveal coordination environment and oxidation state information in metal-based oxidation-reduction processes. We have used this technique to probe reduction of Eu(III) to Eu(II) in Eu-$\alpha1$ and believe that it would be especially useful for the determination of the oxidation states and coordination environments of ^{99}Tc within these POM complexes. In fact it is a technique that can be relied upon for a variety of redox active metals that shuttle between oxidation states.

CONCLUSION

This study aims to understand parameters that stabilize low valent technetium, specifically Tc(IV). Tc(IV) as the TcO_2 species is considered to be relatively immobile compared to pertechnetate, $Tc^{VII}O_4^-$, that is mobile in the environment. The strategy is to employ Tc^VO POMs to access the Tc(IV) oxidation state and assess stabilities of Tc(IV) in different steric and electronic environments. Also, this study identifies other viable oxidation states for Tc(VI, V, IV, III) in the POM matrices. In addition we compare the redox properties of Tc and Re to highlight the differences.

Electrochemistry studies of M^VO-$\boldsymbol{\alpha 1}$ and M^VO-$\boldsymbol{\alpha 2}$ (M = Tc and Re) complexes under a variety of pH conditions show that the Tc-containing derivatives are always more readily reduced than their Re analogues, as expected from elemental periodic properties. Both Tc and Re are reduced more readily in the lacunary $\alpha 1$ site as compared to the $\alpha 2$ site. The $Tc^{V/IV}$ reduction in the $\alpha 1$ site is proton independent compared to the Tc^VO-$\alpha 2$. This feature is consistent with the structure of the M^VO-$\alpha 1$ determined by XAS. EXAFS and XANES data reveal that the Tc^V is "pulled" into the -$\alpha 1$ framework.[27] This may facilitate the reduction of Tc^VO-$\boldsymbol{\alpha 1}$ and stabilization of lower Tc oxidation states. The less electrophilic nature of Tc(V) in Tc^VO-$\boldsymbol{\alpha 1}$ compared to Tc^VO-$\boldsymbol{\alpha 2}$, according to XANES, is consistent with the proton independence of the $Tc^{V/IV}$ reduction process in the former. The DFT calculations, consistent with the electrochemistry, argue that the $\pi^*(Tc{=}O)$ LUMO is lower in energy than the W orbitals for Tc^VO-$\boldsymbol{\alpha 1}$ requiring no protonation to accompany the $Tc^{V/IV}$ reduction. In contrast, the $M^{V/IV}$ reduction process must occur hand in hand with protonation of the terminal M=O for Re^VO-$\boldsymbol{\alpha 1}$ and M^VO-$\boldsymbol{\alpha 2}$ (M = Tc and Re) to make the $\pi^*(M{=}O)$ orbitals accessible to the addition of electrons. It is clear that the electron transfer properties between the $\alpha 1$ and $\alpha 2$ sites are unmistakably different and impact the redox properties of Tc substituted into these defects.

DFT calculations also demonstrate that Tc-containing derivatives are always more readily reduced than their Re analogues because the electrons added upon reduction always occupy lower energy orbitals in the Tc compared to the Re compounds. Calculations show that the first Tc-like orbitals are very low in energy and cannot be completely depopulated, explaining why this atom's maximum oxidation state is VI, whereas in the Re case an oxidation state of VII is justified by higher energy d orbitals. However, because W^{VI} and Re^V reduction waves take place at similar potentials, additional experimental and computational studies are needed to unambiguously identify the formation of Re^{IV} species from the electrochemical reduction of Re^V-based POMs.

ASSOCIATED CONTENT

Ⓢ Supporting Information

Further details are given in Figures S1−S6 and Tables S1−S9. This material is available free of charge via the Internet at http://pubs.acs.org.

AUTHOR INFORMATION

Corresponding Author

*E-mail: lfrances@hunter.cuny.edu.

Present Address

∥Institut Lavoisier, UMR8180, Université de Versailles St. Quentin, 45 Avenue des Etats-Unis, 78035 Versailles Cedex, France.

Author Contributions

#Contributed equally to this work.

Notes

The authors declare no competing financial interest.

ACKNOWLEDGMENTS

REFERENCES

(1) Burke, I. T.; Boothman, C.; Lloyd, J. R.; Livens, F. R.; Charnock, J. M.; McBeth, J. M.; Mortimer, R. J. G.; Morris, K. *Environ. Sci. Technol.* **2006**, *40*, 3529.

(2) Burke, I. T.; Boothman, C.; Lloyd, J. R.; Mortimer, R. J. G.; Livens, F. R.; Morris, K. *Environ. Sci. Technol.* **2005**, *39*, 4109.

(3) Istok, J. D.; Senko, J. M.; Krumholz, L. R.; Watson, D.; Bogle, M. A.; Peacock, A.; Chang, Y. J.; White, D. C. *Environ. Sci. Technol.* **2004**, *38*, 468.

(4) Lloyd, J. R.; Sole, V. A.; Van Praagh, C. V. G.; Lovley, D. R. *Appl. Environ. Microbiol.* **2000**, *66*, 3743.

(5) Lukens, W. W.; Bucher, J. J.; Shuh, D. K.; Edelstein, N. M. *Environ. Sci. Technol.* **2005**, *39*, 8064.

(6) Lukens, W. W.; Shuh, D. K.; Schroeder, N. C.; Ashley, K. R. *Environ. Sci. Technol.* **2004**, *38*, 229.

(7) Maes, A.; Geraedts, K.; Bruggeman, C.; Vancluysen, J.; Rossberg, A.; Henning, C. *Environ. Sci. Technol.* **2004**, *38*, 2044.

(8) Stalmans, M.; Maes, A.; Cremers, A. In *Technetium in the Environment*; Desmet, G., Myttenaere, C., Eds.; Elsevier, Appl. Sci. Publ.: New York, 1986; p 91.

(9) Wildung, R. E.; Li, S. W.; Murray, C. J.; Krupka, K. M.; Xie, Y.; Hess, N. J.; Roden, E. E. *FEMS Microbiol. Ecol.* **2004**, *49*, 151.

(10) Beals, D. M.; Hayes, D. W. *Sci. Total Environ.* **1995**, *173*, 101.

(11) Hunt, A. G.; Skinner, T. E. *Hydrogeol. J.* **2010**, *18*, 381.

(12) U.S. Department of Energy, O. o. B. E. S.; http://www.sc.doe.gov/bes/reports/files/ANES_rpt.pdf, 2006; Vol. *2006*.

(13) Khalil, M. Y.; White, W. B. *J. Am. Ceram. Soc.* **1983**, *66*, C197.

(14) Langton, C. A. Challenging Applications for Hydrated and Chemically Reacted Ceramics. In *Proceedings of the Australian Ceramic Society meeting*, Sydney, Australia, July 12, 1988.

(15) Langton, C. A. *Mater. Res. Soc. Symp. Proc.* **1988**, *112*, 61.

(16) Singh, D.; Mandalika, V. R.; Parulekar, S. J.; Wagh, A. S. *J. Nucl. Mater.* **2006**, *348*, 272.

(17) Day, V. W.; Klemperer, W. G. *Science* **1985**, *228*, 533.

(18) Day, V. W.; Klemperer, W. G.; Schwartz, C.; Wang, R.-C. In *Surface Organometallic Chemistry: Molecular Approaches to Surface Catalysis*; Kluwer Academic Publishers: New York, 1988; p 173.

(19) Fang, X.; Hill, C. L. *Angew. Chem., Int. Ed.* **2007**, *46*, 3877.

(20) Long, D.-L.; Burkholder, E.; Cronin, L. *Chem. Soc. Rev.* **2007**, *36*, 105.

(21) Burton-Pye, B. P.; Radivojevic, I.; McGregor, D.; Mbomekalle, I. M.; Lukens, W. W.; Francesconi, L. C. *J. Am. Chem. Soc.* **2011**, *133* (46), 18802−18815.

(22) Ciabrini, J.-P.; Contant, R. *J. Chem. Res. (M).* **1993**, 2720.

(23) Contant, R.; Abbessi, M.; Canny, J.; Belhouari, A.; Keita, B.; Nadjo, L. *Inorg. Chem.* **1997**, *36*, 4961.

(24) Contant, R.; Herve, G. *Rev. Inorg. Chem.* **2002**, *22*, 63.

(25) Contant, R.; Richet, M.; Lu, Y. W.; Keita, B.; Nadjo, L. *Eur. J. Inorg. Chem.* **2002**, 2587.

(26) Contant, R.; Thouvenot, R. *Inorg. Chim. Acta* **1993**, *212*, 41.

(27) McGregor, D.; Burton-Pye, B. P.; Howell, R. C.; Mbomekalle, I. M.; Lukens, W. W.; Bian, F.; Mausolf, E.; Poineau, F.; Czerwinski, K. R.; Francesconi, L. C. *Inorg. Chem.* **2011**, *50*, 1670.

(28) Lopez, X.; Miro, P.; Carbo, J. J.; Rodriguez-Fortea, A.; Bo, C.; Poblet, J. M. *Theor. Chem. Acc.* **2011**, *128*, 393.

(29) Poblet, J. M.; Lopez, X.; Bo, C. *Chem. Soc. Rev.* **2003**, *32*, 297.

(30) *The inorganic chemistry of technetium and rhenium as relevant to nuclear medicine*; Deutsch, E., Libson, K., Vanderheyden, J.-L., Eds.; Cortina International: Verona, Italy, 1990; Vol. 3.

(31) Libson, K.; Helm, L.; Roodt, A.; Cutler, C.; Merbach, A. E.; Sullivan, J. C.; Deutch, E. *Kinetics and mechanism of ligand substitution on analogous technetium(V) and rhenium(V) complexes*, 3rd ed.; Cortina International: Verona, Italy, 1989.

(32) Libson, K.; Woods, M.; Sullivan, J.; Watkins, J. W., II; Elder, R. C.; Deutsch, E. *Inorg. Chem.* **1988**, *27*, 999.

(33) VanderHeyden, J.-L.; Heeg, M. J.; Deutsch, E. A. *Inorg. Chem.* **1985**, *24*, 1666.

(34) Contant, R. *Inorg. Synth.* **1990**, *27*, 71.

(35) Bartis, J.; Kunina, Y.; Blumenstein, M.; Francesconi, L. C. *Inorg. Chem.* **1996**, *35*, 1497.

(36) Venturelli, A.; Nilges, M. J.; Smirnov, A.; Belford, R. L.; Francesconi, L. C. *J. Chem. Soc., Dalton Trans.* **1999**, 301.

(37) Keita, B.; Girard, F.; Nadjo, L.; Contant, R.; Belghiche, R.; Albessi, M. *J. Electroanal. Chem.* **2001**, *508*, 70.

(38) Baerends, E. J.; Ellis, D. E.; Ros, P. *Chem. Phys.* **1973**, *2*, 41.

(39) Guerra, C. F.; Snijders, J. G.; Te, V. G.; Baerends, E. J. *Theor. Chem. Acc.* **1998**, *99*, 391.

(40) Te, V. G.; Baerends, E. J. *J. Comput. Phys.* **1992**, *99*, 84.

(41) Te, V. G.; Bickelhaupt, F. M.; Baerends, E. J.; Fonseca, G. C.; Van, G. S. J. A.; Snijders, J. G.; Ziegler, T. *J. Comput. Chem.* **2001**, *22*, 931.

(42) Versluis, L.; Ziegler, T. *J. Chem. Phys.* **1988**, *88*, 322.

(43) Becke, A. D. *J. Chem. Phys.* **1986**, *84*, 4524.

(44) Becke, A. D. *Phys. Rev. A: Gen. Phys.* **1988**, *38*, 3098.

(45) Vosko, S. H.; Wilk, L.; Nusair, M. *Can. J. Phys.* **1980**, *58*, 1200.

(46) Perdew, J. P. *Phys. Rev. B* **1986**, *B33*, 8822.

(47) Perdew, J. P. *Phys. Rev. B* **1986**, *B34*, 7406.

(48) Andzelm, J.; Kolmel, C.; Klamt, A. *J. Chem. Phys.* **1995**, *103*, 9312.

(49) Klamt, A. *J. Phys. Chem.* **1995**, *99*, 2224.

(50) Klamt, A.; Schueuermann, G. *J. Chem. Soc., Perkin Trans. 2* **1993**, 799.

(51) Pye, C. C.; Ziegler, T. *Theor. Chem. Acc.* **1999**, *101*, 396.

(52) Lopez, X.; Bo, C.; Poblet, J. M. *J. Am. Chem. Soc.* **2002**, *124*, 12574.

(53) Lewis, A.; Bumpus, J. A.; Truhlar, D. G.; Cramer, C. J. *J. Chem. Educ.* **2007**, *84*, 934.

(54) Keita, B.; Lu, Y. W.; Nadjo, L.; Contant, R. *Electrochem. Commun.* **2000**, *2*, 720.

(55) Kozik, M.; Baker, L. C. W. *J. Am. Chem. Soc.* **1990**, *112*, 7604.

(56) Kozik, M.; Hammer, C. F.; Baker, L. C. W. *J. Am. Chem. Soc.* **1986**, *108*, 2748.

(57) Acerete, R.; Hammer, C. F.; Baker, L. C. W. *J. Am. Chem. Soc.* **1982**, *104*, 5384.

(58) Ciabrini, J. P.; Contant, R.; Fruchart, J. M. *Polyhedron* **1983**, *2*, 1229.

(59) Keita, B.; Girard, F.; Nadjo, L.; Contant, R.; Canny, J.; Richet, M. *J. Electroanal. Chem.* **1999**, *478*, 76.

(60) Contant, R.; Ciabrini, J.-P. *J. Chem. Res. (M)* **1977**, *M*, 2601.

(61) Contant, R.; Ciabrini, J.-P. *J. Chem. Res (M)* **1982**, *1982*, 641.

(62) Keita, B.; Belhouari, A.; Nadjo, L.; Contant, R. *J. Electroanal. Chem.* **1998**, *442*, 49.

(63) Keita, B.; Levy, B.; Nadjo, L.; Contant, R. *New. J. Chem.* **2002**, *26*, 1314.

(64) Keita, B.; Mbomekalle, I.-M.; Nadjo, L.; Contant, R. *Eur. J. Inorg. Chem.* **2002**, 473.

(65) Ortega, F.; Pope, M. T. *Inorg. Chem.* **1984**, *23*, 3292.

(66) Lewis, A.; Bumpus, J. A.; Truhlar, D. G.; Cramer, C. J. *J. Chem. Educ.* **2004**, *81*, 596.

(67) Schwochau, K. *Technetium Chemistry and Radiopharmaceutical Applications*, 1st ed.; Wiley-VCH: Weinheim, Germany, 2000.

(68) Burton-Pye, B. P.; McGregor, D.; Lukens, W. W., Jr.; Francesconi, L. C., manuscript in preparation, 2012.

(69) Jing, J.; Burton-Pye, B. P.; Francesconi, L. C.; Antonio, M. R. *Inorg. Chem.* **2008**, *47*, 6889.